DESIGN AND IMPLEMENTATION OF A PRACTICAL DIRECTION FINDING RECEIVER

H. Peng[*], Z. Q. Yang, and T. Yang

School of Electronic Engineering, University of Electronic Science and Technology of China, Chengdu, Sichuan 611731, China

Abstract—This paper presents a practical direction finding receiver based on six-port networks. To expand beam direction angles, improve measurement accuracy, and avoid phase ambiguity, we introduce a dual-baseline architecture into the direction finding receiver. We also propose a calibration technique based on support vector regression (SVR) for the following reasons: The nonlinearity of diode detectors and the asymmetry of six-port junctions can cause measurement phase errors. Moreover, the transmission parameters of two microwave channels differ with changes in received power. Results show that the SVR model can achieve a direction finding accuracy of $0.2932°$.

1. INTRODUCTION

In modern electronic technology, one of the most important functions of a radar system is detecting a space radiation source. Direction finding receivers have two types of architecture: superheterodyne [1] and zero-intermediate frequency architectures [2–5]. The zero-IF architecture can reduce the cost and size of receivers; thus, direction finding receivers with this type of architecture have been used in measurement systems. The key modules in these receivers are called six-port networks.

In contrast to digital direction finding receivers, the analog types based on six-port networks can detect a narrower pulse width (less than 50 ns). However, the nonlinearity of diode detectors and asymmetry of six-port junctions can both cause measurement errors. Moreover, the transmission parameters of two microwave channels differ with changes in received power. Therefore, a calibration technique is needed to improve the performance of analog direction finding receivers.

Researchers have proposed calibration techniques that are based on artificial neural networks (ANNs) for six-port networks [6] and direction finding receivers [2]. ANNs have been successfully applied in artificial intelligence, device modeling [7, 8], parameter prediction, cognitive science, and other scientific fields. Nevertheless, ANN models suffer from the following drawbacks: multiple local minima, over-fitting, and low generalizability [9]. In this paper, we propose a calibration technique based on support vector regression (SVR). Support vector machine (SVM) theory has generated fruitful results in data classification and regression [10–13]. SVM embodies the structural risk minimization (SRM) principle instead of the traditional empirical risk minimization (ERM) of ANNs. In addition, SVM is a small-sample statistical learning machine that can identify global minima [14].

In practice, dual-baseline or multi-baseline architectures simultaneously satisfy the requirements for measurement accuracy and wide incidence angles. The direction finding principle in these architectures is based on the combination of long and short baselines. Measurement accuracy primarily depends on the long baseline, and phase ambiguity removal depends on the short baseline. Changes in received power can cause I/Q voltages to fluctuate primarily because two microwave channels can't have the same electrical properties. The phase differences between two channels are associated with received power.

In contrast to [2], a dual-baseline architecture and a power detector are added in the direction finding system in current work. Meanwhile, an effective SVR model, instead of ANN, is proposed as calibration technique. The rest of the paper is organized as follows. In Section 2, we discuss the principle underlying direction finding receivers. In Section 3, we present the detailed system design, which includes antennas, microwave circuits, a signal processor, and other modules. A calibration method based on an SVR model is described and demonstrated in Section 4. Section 5 concludes this paper.

2. DIRECTION FINDING RECEIVER PRINCIPLE

The principle of a direction finding receiver for wide beam direction angles is discussed in this section. Figure 1 shows the block diagram of the receiver.

2.1. System Architecture

Figure 1 shows that the receiver consists of three spiral antennas, three limiting amplifier modules, four filters, three power dividers, two phase

discriminator modules, a digital frequency measurement module, a power detection module, and other modules.

Spiral antennas are characterized by wide beamwidths and low gains. It is the reason why direction finding receivers are usually equipped with these antennas.

The limiting amplifier modules include three ports: one input port, one output port, and one coupled output port. The output power of the limiting amplifier module roughly maintains a constant value via a saturated amplifier for different input power levels and signal frequencies. The detection of signal power depends on a linear amplifier, a 10 dB coupler, and a logarithmic amplifier. Four filters are used to further suppress interference and out-of-band white noise.

The phase difference detector consists of a six-port junction, four diodes, and two differential amplifiers. Two detection modules are used in a dual-baseline architecture, and two I/Q signals are simultaneously acquired. Phase discriminator 1 detects the phase difference between the first and third channels, while phase discriminator 2 detects the phase difference between the second and third channels.

Compared with the analog frequency measurement, the digital frequency measurement of radar pulse presents the advantages of versatility, miniaturization and software definition. This direction
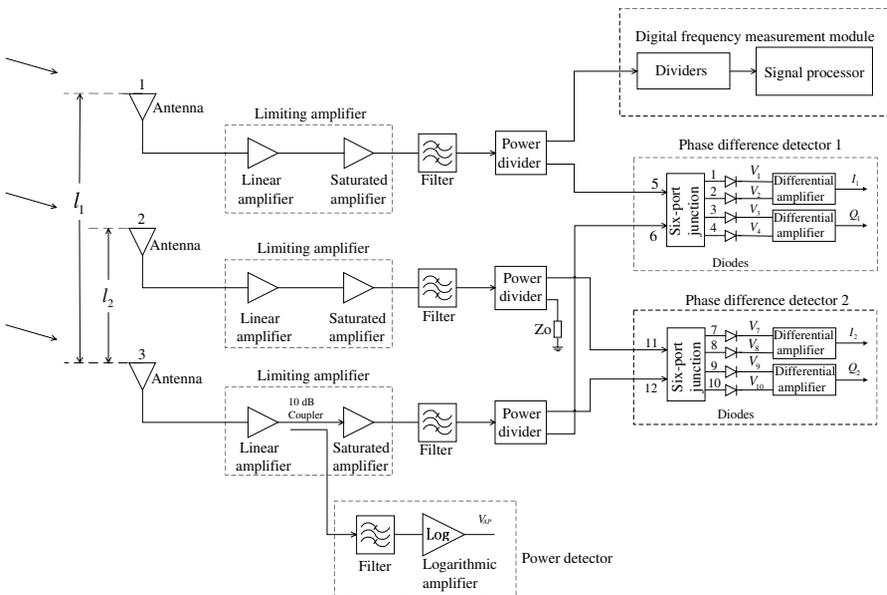

Figure 1. Block diagram of a direction finding receiver for wide beam direction angles.

finding receiver operates at a frequency range of 5–6 GHz. Therefore, a multi-stage divider module is placed between the power divider and signal processor. The divider module consists of one programmable divider ($N = 8$) and two divide-by-2 static dividers. The output frequency of the divider module ranges from 5 GHz/32 = 156.25 MHz to 6 GHz/32 = 187.5 MHz. The digital pulse frequency measurement module, which is based on an equally accurate measurement frequency for counting the number of pulses within a certain period, is applicable to instantaneous frequency measurement in pulse radars.

2.2. Principle of Dual-baseline Interferometer

Figure 2 shows a one-dimensional M-baseline interferometer with baseline length l_i $(i = 1, 2, \ldots M)$. The beam direction angle is θ and the signal wavelength is λ [15].

The relationships between θ, phase differences ϕ_i, and l_i can be expressed as follows:

$$\phi_1 = \frac{l_1}{l_2} \cdot (\phi_2 + 2\pi \cdot K_2) = \ldots = \frac{l_1}{l_i} \cdot (\phi_i + 2\pi \cdot K_i) \, (i = 1, 2, \ldots M) \, (1)$$

$$\phi_i = \frac{l_i \cdot \sin\theta}{\lambda} \cdot 2\pi - 2\pi \cdot K_i (i = 1, 2, \ldots M, K_i = 0, 1, 2, \ldots) \qquad (2)$$

$$K_i = \frac{\frac{l_i \cdot \sin\theta}{\lambda} \cdot 2\pi - \text{mod}\left(\frac{l_i \cdot \sin\theta}{\lambda} \cdot 2\pi \, , \, 2\pi\right)}{2\pi} \qquad (3)$$

Given that shortest baseline l_1 is used to eliminate phase ambiguity, phase differences ϕ_1 should satisfy the following requirement:

$$0 \le \phi_1 < \pi \qquad (4)$$

We will discuss a one-dimensional dual-baseline interferometer. Equations (1), (2), and (3) can be simplified thus:

$$\phi_1 = \frac{l_1}{l_2} \cdot \left[\phi_2 + \frac{l_2 \cdot \sin\theta}{\lambda} \cdot 2\pi - \text{mod}\left(\frac{l_2 \cdot \sin\theta}{\lambda} \cdot 2\pi \, , \, 2\pi\right)\right] \quad (5)$$

$$\phi_1 = \frac{l_1 \cdot \sin\theta}{\lambda} \cdot 2\pi \qquad (6)$$

$$\phi_2 = \text{mod}\left(\frac{l_2 \cdot \sin\theta}{\lambda} \cdot 2\pi \, , \, 2\pi\right) \qquad (7)$$

ϕ_1, which corresponds to l_1, should satisfy the conditions in Equation (4). Long baseline l_2 determines the accuracy with which phase difference is measured. In theory, a longer baseline translates to a higher accuracy. In engineering practice, the ratio of baseline length is about 0.4 to 0.25.
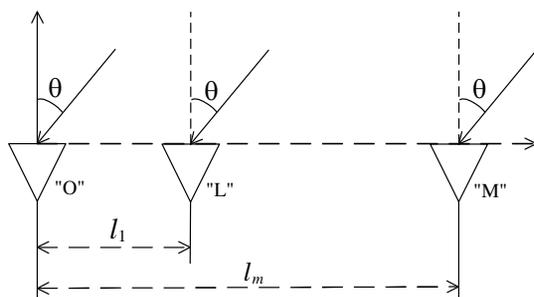
Figure 2. Multi-baseline interferometer.

2.3. Principle of Phase Discriminator

The phase differences of two signals can be calculated using the I/Q amplitudes, and can be expressed as follows [16]:

$$V_n = K_1 \cdot A_1 \cdot B_1 \left[1 + (-1)^n \cdot \cos\left(\phi_1 + j \cdot \pi/2\right)\right]/2$$
$$\begin{cases} j = 0, & \text{if } n = 1, 2 \\ j = -1, & \text{if } n = 3, 4 \end{cases} \tag{8}$$

$$V_n = K_2 \cdot A_2 \cdot B_2 \left[1 + (-1)^n \cdot \cos\left(\phi_2 + j \cdot \pi/2\right)\right]/2$$
$$\begin{cases} j = 0, & \text{if } n = 7, 8 \\ j = -1, & \text{if } n = 9, 10 \end{cases} \tag{9}$$

$$\phi_1 = \tan^{-1}\left(\frac{V_2 - V_1}{V_4 - V_3}\right) \tag{10}$$

$$\phi_2 = \tan^{-1}\left(\frac{V_8 - V_7}{V_{10} - V_9}\right) \tag{11}$$

where V_n is the output voltage of the phase difference detector; K_1, K_2 are constant factors; A_1, B_1, A_2, and B_2 denote the amplitudes of the input signals of six-port networks; n is the correlator output port index; ϕ_1 and ϕ_2 represent the phase differences between the injected signals of six-port networks.

Equations (10) and (11) show that phase differences ϕ_1 and ϕ_2 are unrelated to the absolute amplitudes of input signals. In engineering practice, the power difference of two signals injected into a six-port network is less than 3 dB.

2.4. Analysis

The beam direction angles appear to be easily calculated with Equations (6)–(11), but this assumption overlooks the effect of phase errors, differences in the transmission parameters of two microwave

channels at varied received power levels, and frequency measurement errors. In a practical direction finding system, a dual-baseline architecture simultaneously expands beam direction angles, improves measurement accuracy, and avoids phase ambiguity. The accurate evaluation of beam direction angles depends on the I/Q amplitudes, signal frequency, and input power. The explicit function of θ is difficult to obtain. Its implicit function, however, can be expressed as follows:

$$\theta = f\left[(V_2 - V_1), (V_4 - V_3), (V_8 - V_7), (V_{10} - V_9), V_{AP}, f\right] \qquad (12)$$

where $f(\cdot)$ is a real nonlinear function, and V_{AP} denotes the output voltage of a power detector.

3. SYSTEM DESIGN

A practical direction finding receiver is developed to demonstrate the accuracy of the SVR model. This system, which is tested in an anechoic chamber, comprises one transmitting antenna, three receiving antennas, three limiting amplifiers, three modules of filters and power dividers, two six-port junctions, eight detectors, two operation amplifiers, a power detector, a divider module, and a signal processor, among others.

The direction finding system adopts the pulsed mode operation. A RF signal generator (R&S: SMB100A), the maximum output power of which is up to +25 dBm, is used. A trigger signal of the generator is injected into the signal processor. The pulse voltages of the I/Q signals can be directly displayed on the digital oscilloscope.

The largest dimension of transmitting antenna is about 70 mm, and the distance between the transmitting and receiving antennas is about 1400 mm for a far-field region. The distance between the centers of antennas 1 and 2 is set to $l_1 = 34$ mm, and the distance between the centers of antennas 1 and 3 is set to $l_2 = 100$ mm. A pyramidal horn antenna is used as the transmitting antenna. The gain of the transmitting antenna is greater than 10 dBi, and a 3 dB main beamwidth of $\pm 25°$ is realized. Three spiral antennas are used as the receiving antennas. The gain of the receiving antennas is typically less than 2 dBi, and a 3 dB main beamwidth of $\pm 60°$ is realized.

The output power of the limiting amplifier is maintained at roughly 8 dBm (input power: -55 to -20 dBm), and the output power of the coupler ranges from -45 to -10 dBm. The noise of the limiting amplifier is about 2 dB. For the detectors working at the square-law region, the output voltages are less than 70 mV. To enable fast and accurate frequency measurements, a multi-stage frequency divider module is developed. The first and the third

stages (dividing by two) consist of two static frequency divider chips (HMC361S8G), which is realized in InGaP GaAs HBT (heterojunction bipolar transistor) technology. The second stage (dividing by eight) uses one programmable frequency divider chip (HMC705LP4). The output frequency of the divider module is $5\,\mathrm{GHz}/32 = 156.25\,\mathrm{MHz}$ to $6\,\mathrm{GHz}/32 = 187.5\,\mathrm{MHz}$.

Except for the custom limiting amplifiers and detectors, the other microwave circuits are all realized on a Taconic-TLX-8 ($h = 0.79\,\mathrm{mm}$, $\varepsilon_r = 2.55$). The key component of a signal processor, which is fabricated on an FR4 ($h = 1.5\,\mathrm{mm}$, 4 layers), is the Altera Stratix II FPGA. The trigger signal is used to determine the start and ending point of frequency measurement.

Figure 3 shows the test platform in the anechoic chamber.

The beam direction angles are set as $-36°$ to $36°$ at $3°$ intervals. The output power of signal generator is set as -5 to $25\,\mathrm{dBm}$ at $10\,\mathrm{dB}$ intervals, and the frequencies are set as 5 to $6\,\mathrm{GHz}$ at $200\,\mathrm{MHz}$ intervals. The transmission parameter from the transmitting antenna to the receiving antenna is about $-46\,\mathrm{dB}$. Therefore, the receiving power is about -51 to $-21\,\mathrm{dBm}$ at $10\,\mathrm{dB}$ intervals. Three receiving antennas are fixed at a rotary table.
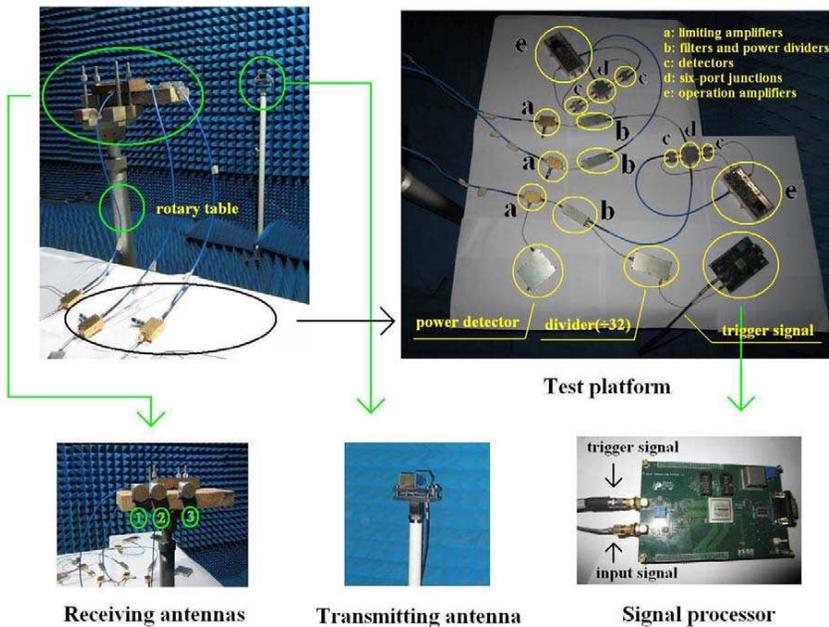

Figure 3. Test platform in the anechoic chamber.

4. CALIBRATION OF SVR MODEL

A total of 600 standards are established, and all readings $(I_1, Q_1, I_2, Q_2, V_{AP}, f)$ are measured and recorded. Two-thirds of the data (400 samples) are randomly selected as the training data set, and the rest are classified as the cross-validation data set (200 samples).

Vapnik proposed SVM theory in 1995 [17], and since then been successfully applied in data regression. It embodies the SRM principle and is a small-sample statistical learning machine. In theory, this method always identifies global minima. Chang and Lin developed the Library for SVM toolbox to calculate various models [18]. The following SVR parameters should first be obtained: the constant definition of kernel function (γ), tolerance of termination criterion (ε), penalty parameter (C), and constant ν. $\nu \in [0, 1]$ is the parameter that controls the number of support vectors. The K-fold Cross-Validation (K-CV) method [19], which was also applied in our previous work [13], is used to calculate the optimal parameters of γ and C. The SVR parameters are as follows: $\varepsilon = 0.0001$, $\nu = 0.1$, $C = 0.965936$, and $\gamma = 0.5$. The Root Mean Square Error (RMSE) and Pearson Product-Moment correlation coefficient (R) are calculated to determine the accuracy of the SVR model. RMSE and R are expressed as:

$$\text{RMSE} = \sqrt{\frac{1}{N} \sum_{i=1}^{N} (a_i - b_i)^2} \tag{13}$$

$$R = \frac{\sum\limits_{i=1}^{N} \left(b_i - \overline{b}\right) (a_i - \overline{a})}{\sqrt{\sum\limits_{i=1}^{N} \left(b_i - \overline{b}\right)^2 \sum\limits_{i=1}^{N} (a_i - \overline{a})^2}} \tag{14}$$

where a_i is the predicted beam direction angle of the training or cross-validation data set based on the SVR model; $\overline{a}$ denotes the mean of the predicted beam direction angle of the training or cross-validation data set; b_i is the real beam direction angle; $\overline{b}$ represents mean of the real beam direction angle; N is the data number.

For the training data set, the RMSE of the beam direction angle is $0.1733°$ over the $-36°$ to $36°$ range. The fresh cross-validation data set (200 samples) is used to determine the accuracy of the proposed SVR model. For the cross-validation data set, the RMSE is $0.2932°$ over the range of $-36°$ to $36°$. These results are summarized in Table 1, which indicates that the SVR model predicts the results well.

Figure 4 shows the absolute errors (°) and indicates that the absolute errors of most predicted results are less than $\pm0.5°$.

Table 1. RMSE and R of the training and cross-validation data sets.

	Training Data Set (400 samples)	Cross-Validation Data Set (200 samples)
RMSE	**0.1733°**	**0.2932°**
R	**0.99997**	**0.99991**

$N = 200$
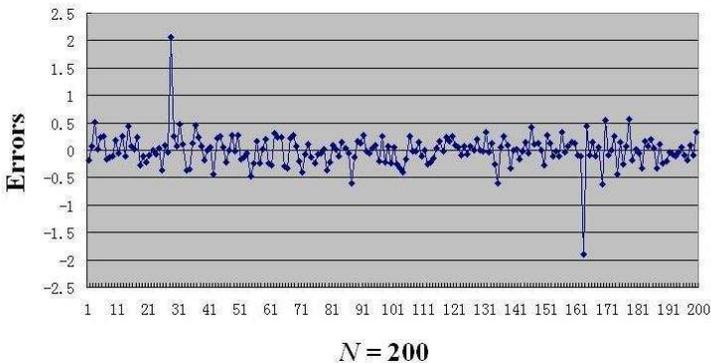
Figure 4. Error statistics.

5. CONCLUSION

Researchers have used the single-baseline principle as basis in calibrating direction finding receivers at fixed power levels. In current work, for expansion of beam direction angles and phase compensation of channels, a dual-baseline interferometer and a power detector are incorporated into the system. The advantages of calibration technique include a higher accuracy, less stringent requirements on the linearity and uniformity of the components, such as the diode detectors, six-port junctions, etc.. Meanwhile, it is very simple to implement in mathematical software. An effective SVR model, instead of ANN, is proposed for calibrating the beam direction angles. The calibration result exhibits an RMSE of 0.2932°.

ACKNOWLEDGMENT

REFERENCES

1. FaIk, J., P. Handel, and M. Jansson, "Effects of frequency and phase errors in electronic warfare TDOA direction-finding systems," *Military Communications Conference, MILCOM*, Boston, United States, Oct. 2003.

2. Peng, H., Z. Yang, and T. Yang, "Calibration of a six-port receiver for direction finding using the artificial neural network technique," *Progress In Electromagnetics Research Letters*, Vol. 27, 17–24, 2011.

3. Huyart, B., J.-J. Laurin, R. G. Bosisio, and D. Roscoe, "A direction-finding antenna system using an integrated six-port circuit," *IEEE Trans. Antennas Propagation*, Vol. 43, No. 12, 1508–1512, Dec. 1995.

4. Yakabe, T., F. Xiao, K. Iwamoto, F. M. Ghannouchi, K. Fujii, and H. Yabe, "Six-port based wave-correlator with application to beam direction finding," *IEEE Trans. Instrum. Meas.*, Vol. 50, No. 2, 377–380, Apr. 2001.

5. Vinci, G., A. Koelpin, and R. Weigel, "Employing six-port technology for phase-measurement-based calibration of automotive radar," *Microwave Conference, APMC*, Singapore, Dec. 2009.

6. Liu, Y., "Calibrating an industrial microwave six-port instrument using the artificial neural network technique," *IEEE Trans. Instrum. Meas.*, Vol. 45, No. 2, 651–656, Apr. 1996.

7. Li, X., Y. Li, and J. Zhao, "Ann-based pad modeling technique for mosfet devices," *Progress In Electromagnetics Research*, Vol. 118, 303–319, 2011.

8. Yang, Z. Q., T. Yang, and Y. Liu, "Design of microstrip lange coupler based on EM-ANN model," *International Journal of Infrared and Millimeter Waves*, Vol. 27, 1381–1389, 2006.

9. Chen, K., C. Ho, and H. Shiau, "Application of support vector regression in forecasting international tourism demand," *Tourism Management Research*, Vol. 4, 81–97, 2004.

10. Yang, Z. Q., T. Yang, Y. Liu, and S. H. Han, "MIM capacitor modeling by support vector regression," *Journal of Electromagnetic Waves and Applications*, Vol. 22, No. 1, 61–67, 2008.

11. Wei, C., J. O. Chong, and S. S. Keerthi, "An improved conjugate gradient scheme to the solution of least squares SVM," *IEEE Trans. Neural Network*, Vol. 6, 498–501, Mar. 2005.

12. Xia, L., R. Xu, and B. Yan, "LTCC interconnect modeling

by support vector regression," *Progress In Electromagnetics Research*, Vol. 69, 67–75, 2007.

13. Peng, H., Z. Yang, and T. Yang, "Calibration of a six-port position sensor via support vector regression," *Progress In Electromagnetics Research C*, Vol. 26, 71–81, 2012.

14. Bermani, E., A. Boni, A. Kerhet, and A. Massa, "Kernels evaluation of SVM-based estimators for inverse scattering problems," *Progress In Electromagnetics Research*, Vol. 53, 167–188, 2005.

15. Zheng, W., X. G. Zuo, Y. K. Ma, and Z. S. Hou, "Algorithm of multi-baseline interferometer phase difference in fuzzy circumstance" *International Conference on Consumer Electronics, Communications and Networks (CECNet)*, Xianning, China, Apr. 2011.

16. Cicolani, M. and F. Marchetti, "Phase and amplitude automatic measurements on pulsed RF signals," *Twenty-second European Microwave Conference*, Helsinki, Finland, Sept. 1992.

17. Vapnik, V., *The Nature of Statistical Learning Theory*, Springer-Verlag, New York, 1995.

18. Chang, C. C. and C. J. Lin, "LIBSVM: A library for support vector machines," System documentation, National Taiwan University, 2004.

19. Bengio, Y. and Y. Grandvalet, "No unbiased estimator of the variance of K-fold cross-validation," *J. Machine Learning Research*, Vol. 5, 1089–1105, 2004.